# Mechanistic Origin of the Correlation between Spin State and Spectra of Model Cytochrome P450 Ferric Heme Proteins

**Danni Harris* and Gilda Loew**

*Contribution from the Molecular Research Institute, 845 Page Mill Road, Palo Alto, California 94304*

*Received November 9, 1992*

**Abstract:** We report here the use of the semiempirical quantum chemical INDO/ROHF/CI method to calculate the electronic structure and optical spectra of the high- and low-spin states of the active site of the substrate-free form of cytochrome $P450_{cam}$. The goal of these studies was to determine whether there is an underlying mechanism coupling the spin-state change itself with the observed shifts in the optical spectra, in the absence of any other changes in the heme unit. UV–visible spectroscopy, specifically, a small shift in the Soret band, is routinely used in empirical correlations to determine the variation in percent high-spin and low-spin forms as a function of a specific change in heme proteins, for example, in the axial ligands, in the substrate binding, or in a mutant. These correlations are weakened, however, by the lack of a mechanistic link between the two properties and because it is possible that the observed Soret band shifts are caused directly by the differences between the two heme proteins being compared without the intermediacy of a spin-state change. Comparison of the calculated spectra of the two spin states reveals that, upon change of the Fe(III) from a low- to a high-spin reference state, a blue shift does indeed occur in the strong Soret band absorptions found in the 25 000 $cm^{-1}$ region that consists primarily of porphyrin $\pi$–$\pi^*$ transitions. These results establish that a spin-state change alone leads to the observed shift in the Soret band. They also elucidate the origin of the observed shift in the Soret band and show it to be a direct consequence of the spin-state change. In the low-spin state, there is enhanced mixing of the iron d (eg) and porphyrin 4eg ($\pi^*$) orbitals, resulting in a lowering of the eg($\pi^*$) states, and a consequent shift to the red of the Soret band, clearly demonstrating an underlying physical basis for the observed correlation between ferric heme spin state and measured spectral shifts associated with ($\pi \rightarrow \pi^*$) heme transitions.

## Introduction

The spin-state change which occurs upon substrate binding of camphor in cytochrome P450 monooxygenase from the bacterium *Pseudomonas putida* ($P450_{cam}$) has been shown to be functionally important in the enzymatic cycle of this enzyme. The change from low-spin to high-spin state, upon binding of hydrophobic substrates, has a significant effect on the subsequent redox equilibria. The redox potential shifts from −340 mV in the substrate-free to −173 mV in the camphor-bound cytochrome P450, allowing facile one-electron reduction, which is the next step in the enzymatic cycle leading to the catalytically active form. Thus, characterization of the percentage of high-spin form resulting from binding of different substrates or from mutations of the enzyme has become a commonly used indicator of enzymatic efficiency.

The determination of the spin multiplicity of the ground state of heme proteins is a particularly challenging task since they typically have a number of very low energy states of differing multiplicities. For example, ferriheme proteins have low-lying sextet, quartet, and doublet states, and ferrous heme proteins have low-lying quintet, triplet, and singlet states. Moreover, the relative energies of these different states are very sensitive to small changes in the heme environment, such as variations in the axial ligands and the extent of out-of-planarity of the iron, so that changes in ground-state multiplicity readily occur.

The most direct measure of the ground-state spin and of the presence of energy-accessible states of different multiplicities are temperature-dependent magnetic susceptibility measurements and, for ferriheme systems, electron spin resonance spectra. However, these measurements are complex and do not readily lend themselves to monitoring during the course of a time-dependent change in the system, for example, titration of an enzyme with a substrate or inhibitor.

A practical solution to this problem was found when features of the two dominant bands in the optical spectra of heme proteins were shown to correlate with iron spin states independently measured by magnetic susceptibilities in metmyoglobin,[1] ferrimyoglobin (horse heart), ferrihemoglobin (horse erythrocyte and *Chironomus plumosos*), and peroxidase (horseradish).[2] The UV–visible spectra of metalloporphyrins are dominated by two bands, called Q and B (Soret).[3] They have been interpreted as largely porphyrin ($\pi \rightarrow \pi^*$) in origin, with the major transitions occurring between the highest occupied $3a_{2u}$ and $1a_{1u}$ orbitals to the lowest unoccupied 4eg($\pi^*$) orbitals. The B (Soret) bands are the most intense and are generally found between 380 and 420 nm, with molar extinction coefficients on the order of $10^5$ $M^{-1}$ $cm^{-1}$. The two Q bands, denoted by $\alpha$ and $\beta$, seen between 500 and 600 nm are much weaker, with extinction coefficients of about $10^4$ $M^{-1}$ $cm^{-1}$. This early work demonstrated that Q-band intensity diminishes and the Soret (B) band position shifts to higher frequency in the high-spin state. Subsequently, Smith and Williams showed that the magnetic susceptibility varied monotonically with Soret band position for myoglobin solutions containing differing anionic ligands.[4] Such a correlation was also more recently ascertained for liver microsomal P450[5] and $P450_{cam}$[6] by independent magnetic susceptibility, electron spin resonance, and optical spectra measurements. Thus, for many years now, a shift in frequency of the Soret band in the UV–visible spectra has been routinely used to quantify the amounts of high- and low-spin forms of heme proteins.

While monitoring a small change in the frequency of the Soret band is a very efficient way of inferring a spin-state change in heme proteins, there are two aspects of this empirical correlation which weaken its validity. The first is that a mechanistic link

(1) Beetlestone, J.; George, P. *Biochemistry* **1964**, *3*, 707.
(2) George, P.; Beetlestone, J.; Griffith, J. S. *Rev. Mod. Phys.* **1964**, *36*, 441.
(3) Platt, J. R. In *Radiation Biology*; Hollaender, A., Ed.; McGraw-Hill: New York, 1956; Vol. III, Chapter 2.
(4) Smith, D. W.; Williams, R. J. P. *Biochem. J.* **1968**, *110*, 297.
(5) Jefcoate, C. R. E.; Gaylor, J. L. *Biochemistry* **1970**, *8*, 3464.
(6) Sligar, S. G. *Biochemistry* **1976**, *15*, 5399.

0002-7863/93/1515-5799$04.00/0 

between the observed blue shift in the Soret band of the optical spectra and a change in the spin state of the iron has yet to be established since optical spectra are not *a priori* a probe of the spin states of a chromophore. The earliest attempt to relate the Soret shift with a spin-state change was performed by Braterman and co-workers in 1964.[7] This early work suggested that the blue shift of the Soret band of a high-spin protein compared to the low-spin form was a result of increased mixing in the high-spin form of charge-transfer $E_u$ excited states $E_u(a_{1u}, d_{xz}, d_{yz})$ and $E_u(a_{2u}, d_{xz}, d_{yz})$ with the $E_u(\pi-\pi^*)$ excited states, shifting the highest of these four mixed states corresponding to the Soret transition to a higher frequency. However, no calculations have been reported to verify this hypothesis.

The second mitigating factor is that, in all cases, Soret band shifts are monitored between two heme proteins that differ in some respect, for example, in axial ligand, substrate, inhibitor, or a site-specific mutation of the protein. Few of the many heme systems thus studied have had both their magnetic and optical properties characterized. Thus, it is possible that the observed shift is a direct result of the difference between the two protein systems being monitored, without the obligatory involvement of a spin-state change.

The goal of this study was to address both of these concerns. To this end, the electronic structure and spectra of the high- and low-spin states of the substrate-free form of cytochrome $P450_{cam}$ have been calculated with the identical model heme active site using semiempirical quantum mechanical methods. The use of the techniques of computational chemistry is ideally suited to determine whether there is an underlying mechanism coupling the spin-state change with the observed shifts in the Soret band of the optical spectra of heme proteins, since calculations can be made for the identical heme complex in both high- and low-spin states without changing any other feature of the heme unit. Such an idealized comparison is possible only in a computer simulation, since in a real system some change has to occur to cause the spin-state change, and one can never completely decouple the two possible sources of the effect on the Soret band. The model used here is the active site of the substrate-free $P450_{cam}$,[8] a cysteine–ferric heme–water complex, as found in the 2.2-Å resolution crystal structure, using the full protoporphyrin IX prosthetic group, with the cysteine residue replaced by methyl mercaptide.

## Methods/Computational Details

The ground-state geometry of the ferric heme–cysteinate system used was extracted from an AMBER 3.0A[9] energy-minimized structure of the substrate-free crystal structure of cytochrome $P450_{cam}$.[8] The heme is attached to the protein in cytochrome $P450_{cam}$ via a cysteinate mercaptide linkage. The iron atom in the cytochrome P450 substrate-free crystal structure is 0.30 Å out of the plane of the porphyrin ring toward the cysteine ligand. Such a displacement has been shown to stabilize the sextet state of the cysteinate–heme–aquo system in the resting state of the enzyme relative to configurations with the iron "in plane".[10] Energy minimization using AMBER resulted in minor changes in the geometry; the iron–water distance is 2.05 Å, and the ferric ion is displaced from the heme core by about 0.25 Å. The cysteinate found in the substrate-free crystal structure was represented in our calculations as a methyl mercaptide. The complex for which calculations were made is shown in Figure 1. Using AMBER 3.0A, hydrogen atoms were added to the heme unit including the

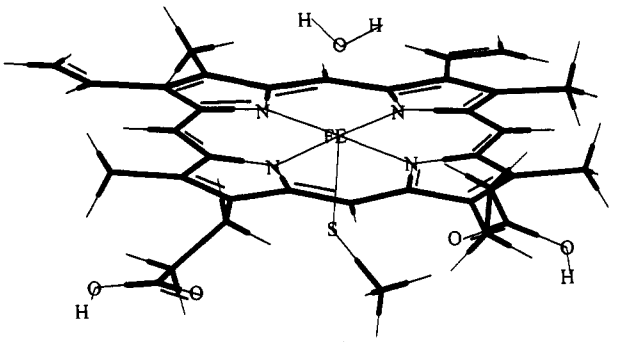

**Figure 1.** Model ferric $P450_{cam}$ site used, based on the coordinates of the cysteinate–ferric heme–water complex of substrate-free cytochrome $P450_{cam}$ ($Fe-OH_2$ = 2.05 Å, Fe–S = 2.24 Å).

propionate substituents of the protoporphyrin IX heme prosthetic group, converting it to neutral propionic acid to simulate the effect of H-bonding to proton-donating residues in the protein.

Semiempirical calculations were performed to characterize the electronic structure and relative energies of the sextet and doublet states of the model $P450_{cam}$ active site and their electronic spectra. In these studies, an INDO-based restricted open-shell Fock configuration interaction formalism (INDO/ROHF/CI) was used, as described in detail elsewhere.[11] The electronic configurations of the Fe(III) center used were the $d_{xy}^1d_{xz}^1d_{yz}^1(d_{z^2})^1(d_{x^2-y^2})^1$ ($S = {}^5/_2$) and $d_{xy}^2d_{xz}^{1.5}d_{yz}^{1.5}$ ($S = {}^1/_2$). The half-electron representation employed for the doublet state was necessary to minimize the effects due to artifactual "symmetry-breaking" of the doublet ground-state representation in the absence of extensive CI.[12,13]

Electronic absorption spectra of the sextet and doublet states of the mercaptide–ferric heme–aquo complex were obtained by performing single excitation configuration interaction (SCCI) calculations. Electric dipole transition matrix elements were calculated to obtain oscillator strengths. Two reference state determinants ($d_{xy}^2d_{xz}^2d_{yz}^1$ and $d_{xy}^2d_{xz}^1d_{yz}^2$) were utilized to represent the $d_{xy}^2d_{xz}^{1.5}d_{yz}^{1.5}$ symmetrical $d\pi$ doublet $^2Eg$ state, and a single ($d_{xy}^1d_{xz}^1d_{yz}^1(d_{z^2})^1(d_{x^2-y^2})^1$) determinant was used to represent the high-spin ($S = {}^5/_2$; $A_{1g}$) state. The molecular orbitals included in the active space for CI calculations were all of the occupied and virtual iron d-containing orbitals, the porphyrin $\pi$ orbitals $3a_{2u}$, $1a_{1u}$, and 3eg, and the porphyrin $\pi^*$ orbitals 4eg and $2b_{1u}$. Excitations stemming from these filled porphyrin and d orbitals to the unfilled porphyrin and iron d orbitals are the source of all spectra reported.

## Results and Discussion

Figure 2 shows all of the allowed transitions calculated for the model substrate-free $P450_{cam}$ active site (Figure 1) in the $S = {}^5/_2$ and $S = {}^1/_2$ states, respectively, in the frequency range 22 000–32 000 $cm^{-1}$. Tables I and II give the calculated frequencies and oscillator strengths for the dominant peaks (i.e., 10% of the maximum intensity) corresponding to the B- and Q-band systems in the high-spin and low-spin spectra, as well as the percent contribution of different types of molecular orbital excitations to each transition. Transitions were identified as part of the Soret band if they contained at least 10% $1a_{1u},3a_{2u}\rightarrow 4eg(\pi^*)$ excitation character. Clearly evident in Figure 2 is the blue shift of the excitations forming the Soret band in the high-spin complex relative to the low-spin complex. Moreover, the spectral shift between the strongest B-bands in the low-spin and high-spin spectra is from 27 800 to 30 129 $cm^{-1}$, a shift of 29 nm. This calculated shift is in remarkable agreement with the value found from experiment (low-spin, 23 980 $cm^{-1}\rightarrow$high-spin, 25 575 $cm^{-1}$)

(7) Braterman, P. S.; Davies, R. C.; Williams, R. J. P. *Adv. Chem. Phys.* **1964**, *7*, 359.
(8) Poulos, T. L.; Finzel, B. C.; Howard, A. J. *Biochemistry* **1991**, *25*, 5314.
(9) Singh, U. C.; Weiner, P. K.; Caldwell, J. W.; Kollman, P. A. AMBER UCSF Version 3.0a, Department of Pharmaceutical Chemistry, University of California, San Francisco, 1986; Revision A by George Seibel, 1989.
(10) Loew, G. H.; Collins, J.; Luke, B.; Waleh, A.; Pudzianowski, A. *Enzyme* **1986**, *36*, 54.
(11) (a) Edwards, W. D.; Weiner, B.; Zerner, M. C. *J. Am. Chem. Soc.* **1986**, *108*, 2196. (b) Edwards, W. D.; Zerner, M. C. *Theor. Chim. Acta* **1987**, *72*, 347.
(12) Davidson, E. R.; Borden, W. T. *J. Phys. Chem.* **1983**, *87*, 4783.
(13) Du, P.; Loew, G. H. *J. Phys. Chem.* **1991**, *95*, 6379.

**Table I.** Calculated Frequencies, Intensities, and Dominant Transitions in Q- and B-Band Systems for High-Spin ($S = {}^5/_2$) Model P450$_{cam}$

| $\nu$ (cm$^{-1}$) | $f$/polarizn | excitation (%) | excitation character | transition character |
|---|---|---|---|---|
| 15 370 | 0.03/$xy$ | 52.9 | $1a_{1u}(\pi)\rightarrow 4eg(\pi^*)$ | $\pi\rightarrow\pi^*$ |
| | | 39.0 | $3a_{2u}(\pi)\rightarrow 4eg(\pi^*)$ | |
| | | 2.2 | $d_{x^2}\rightarrow 4eg(\pi^*)$ | CT |
| 15 450 | 0.03/$xy$ | 54.2 | $1a_{1u}(\pi)\rightarrow 4eg(\pi^*)$ | $\pi\rightarrow\pi^*$ |
| | | 38.5 | $3a_{2u}(\pi)\rightarrow 4eg(\pi^*)$ | |
| 23 326 | 0.24/$xy$ | 19.0 | $3eg(\pi)\rightarrow 4eg(\pi^*)$ | $\pi\rightarrow\pi^*$ |
| | | 13.4 | $3a_{2u}(\pi)\rightarrow 4eg(\pi^*)$ | |
| | | 13.0 | $1a_{1u}(\pi)\rightarrow 4eg(\pi^*)$ | |
| | | 19.5 | $3a_{2u}(\pi)\rightarrow d_{yz}$ | CT |
| | | 14.2 | $3eg(\pi)\rightarrow d_{z^2}$ | |
| | | 10.3 | $3a_{2u}(\pi)\rightarrow d_{z^2}$ | |
| 23 528 | 0.15/$xy$ | 17.1 | $3eg(\pi)\rightarrow 4eg(\pi^*)$ | $\pi\rightarrow\pi^*$ |
| | | 15.7 | $3a_{2u}(\pi)\rightarrow 4eg(\pi^*)$ | |
| | | 6.5 | $1a_{1u}(\pi)\rightarrow 4eg(\pi^*)$ | |
| | | 19.9 | $3a_{2u}(\pi)\rightarrow d_{z^2}$ | CT |
| | | 14.5 | $d_{z^2}\rightarrow 4eg(\pi^*)$ | |
| | | 10.2 | $3a_{2u}(\pi)\rightarrow d_{xz}$ | |
| | | 5.8 | $3eg(\pi)\rightarrow d_{z^2}$ | |
| | | 3.7 | $3eg(\pi)\rightarrow d_{yz}$ | |
| 23 755 | 0.17/$xy$ | 43.8 | $3eg(\pi)\rightarrow 4eg(\pi^*)$ | $\pi\rightarrow\pi^*$ |
| | | 8.7 | $3a_{2u}(\pi)\rightarrow 4eg(\pi^*)$ | |
| | | 7.6 | $1a_{1u}(\pi)$–$4eg(\pi^*)$ | |
| | | 3.4 | $3eg(\pi)\rightarrow 2b_{1u}(\pi^*)$ | |
| | | 13.4 | $3a_{2u}\rightarrow d_{xz}$ | CT |
| | | 5.5 | $3a_{2u}\rightarrow d_{yz}$ | |
| | | 2.3 | $3eg(\pi)\rightarrow d_{xz}$ | |
| | | 2.1 | $3eg(\pi)\rightarrow d_{yz}$ | |
| 27 754 | 0.25/$xy$ | 27.1 | $3a_{2u}(\pi)\rightarrow 2b_{1u}(\pi^*)$ | $\pi\rightarrow\pi^*$ |
| | | 21.1 | $3eg(\pi)\rightarrow 4eg(\pi^*)$ | |
| | | 16.7 | $3a_{2u}(\pi)\rightarrow 4eg(\pi^*)$ | |
| | | 6.0 | $1a_{1u}(\pi)\rightarrow 4eg(\pi^*)$ | |
| | | 13.8 | $d_{z^2}\rightarrow 4eg(\pi^*)$ | CT |
| | | 4.2 | $3a_{2u}(\pi)\rightarrow d_{yz}$ | |
| | | 2.0 | $3a_{2u}(\pi)\rightarrow d_{xz}$ | |
| 28 199 | 0.40/$xy$ | 40.5 | $3eg(\pi)\rightarrow 4eg(\pi^*)$ | $\pi\rightarrow\pi^*$ |
| | | 16.3 | $3a_{2u}(\pi)\rightarrow 4eg(\pi^*)$ | |
| | | 7.7 | $1a_{1u}(\pi)$–$4eg(\pi^*)$ | |
| | | 9.2 | $3a_{2u}(\pi)\rightarrow d_{yz}$ | CT |
| | | 7.3 | $d_{z^2}\rightarrow 4eg(\pi^*)$ | |
| | | 2.9 | $3a_{2u}(\pi)\rightarrow d_{xz}$ | |
| | | 2.6 | $3a_{2u}(\pi)\rightarrow d_{x^2-y^2}$ | |
| 28 549 | 0.20/$xy$ | 33.1 | $1a_{1u}(\pi)\rightarrow 2b_{1u}(\pi^*)$ | $\pi\rightarrow\pi^*$ |
| | | 28.9 | $3eg(\pi)\rightarrow 4eg(\pi^*)$ | |
| | | 18.0 | $3a_{2u}(\pi)\rightarrow 4eg(\pi^*)$ | |
| | | 3.5 | $3eg(\pi)\rightarrow 2b_{1u}(\pi^*)$ | |
| | | 3.2 | $1a_{1u}(\pi)\rightarrow 4eg(\pi^*)$ | |
| | | 3.8 | $3a_{2u}(\pi)\rightarrow d_{xz}$ | CT |
| | | 2.4 | $d_{x^2}\rightarrow 4eg(\pi^*)$ | |
| 30 129 | 1.0/$xy$ | 30.9 | $3eg(\pi)\rightarrow 4eg(\pi^*)$ | $\pi\rightarrow\pi^*$ |
| | | 24.6 | $3a_{2u}(\pi)\rightarrow 4eg(\pi^*)$ | |
| | | 15.1 | $1a_{1u}(\pi)\rightarrow 2b_{1u}(\pi^*)$ | |
| | | 9.7 | $1a_{1u}(\pi)\rightarrow 4eg(\pi^*)$ | |
| 30 322 | 0.79/$xy$ | 40.6 | $3eg(\pi)\rightarrow 4eg(\pi^*)$ | $\pi\rightarrow\pi^*$ |
| | | 18.2 | $3a_{2u}(\pi)\rightarrow 4eg(\pi^*)$ | |
| | | 18.0 | $1a_{1u}(\pi)\rightarrow 2b_{1u}(\pi^*)$ | |
| | | 6.5 | $1a_{1u}(\pi)\rightarrow 4eg(\pi^*)$ | |
| | | 6.2 | $d_{z^2}\rightarrow 4eg(\pi^*)$ | CT |
| 30 924 | 0.56/$xy$ | 58.7 | $1a_{1u}(\pi)\rightarrow 2b_{1u}(\pi^*)$ | $\pi\rightarrow\pi^*$ |
| | | 18.6 | $3eg(\pi)\rightarrow 4eg(\pi^*)$ | |
| | | 12.0 | $3a_{2u}(\pi)\rightarrow 4eg(\pi^*)$ | |
| | | 6.0 | $1a_{1u}(\pi)\rightarrow 4eg(\pi^*)$ | |
| 31 179 | 0.75/$xy$ | 67.2 | $3eg(\pi)\rightarrow 4eg(\pi^*)$ | $\pi\rightarrow\pi^*$ |
| | | 13.4 | $3a_{2u}(\pi)\rightarrow 4eg(\pi^*)$ | |
| | | 7.1 | $1a_{1u}(\pi)\rightarrow 4eg(\pi^*)$ | |
| | | 3.3 | $1a_{1u}(\pi)\rightarrow 2b_{1u}(\pi^*)$ | |

of 26 nm.[14] Thus, the changes in spectra can be definitively linked to the spin-state change, since no other changes in the system were made. These results then provide striking confirmation, for the first time, that a spin-state change alone leads to the observed shift in Soret band frequency.

(14) Dawson, J. H.; Eble, K. S. *Adv. Inorg. Bioinorg. Mech.* **1986**, *4*, 1.

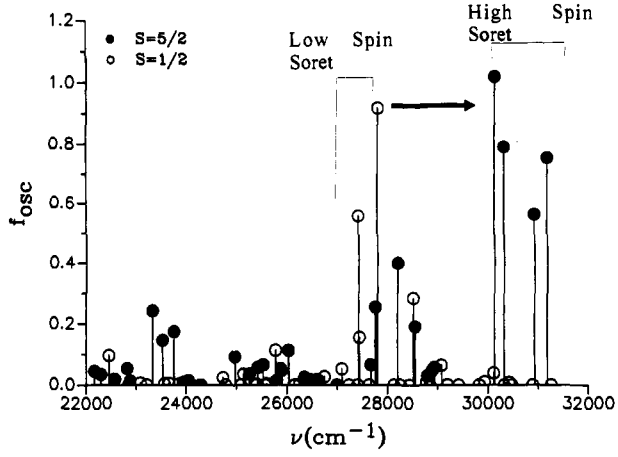


**Figure 2.** Spectrum of the methyl mercaptide–ferric heme–aquo system with an iron–ligand water distance of 2.05 Å. The arrow indicates the shift in the strong $\beta$-bands on a change of the iron spin state from low (○) to high (●) spin. The intensity of the low-spin spectrum has been scaled by 2×.

**Table II.** Calculated Frequencies, Intensities, and Dominant Transitions in Q- and B-Band Systems for Low-Spin ($S = {}^1/_2$) Model P450$_{cam}$

| $\nu$ (cm$^{-1}$) | $f$/polarizn | excitation (%) | excitation character | transition character |
|---|---|---|---|---|
| 16 535 | 0.03/$xy$ | 53.8 | $1a_{1u}(\pi)\rightarrow 4eg(\pi^*)$ | $\pi\rightarrow\pi^*$ |
| | | 37.7 | $3a_{2u}(\pi)\rightarrow 4eg(\pi^*)$ | |
| | | 3.2 | $3a_{2u}(\pi)\rightarrow d_{x^2-y^2}$ | CT |
| 16 552 | 0.03/$xy$ | 49.5 | $1a_{1u}(\pi)\rightarrow 4eg(\pi^*)$ | $\pi\rightarrow\pi^*$ |
| | | 41.5 | $3a_{2u}(\pi)\rightarrow 4eg(\pi^*)$ | |
| | | 3.4 | $3a_{2u}(\pi)\rightarrow d_{x^2-y^2}$ | CT |
| 27 418 | 0.27/$xy$ | 37.7 | $3a_{2u}(\pi)\rightarrow 4eg(\pi^*)$ | $\pi\rightarrow\pi^*$ |
| | | 13.2 | $3eg(\pi)\rightarrow 4eg(\pi^*)$ | |
| | | 8.8 | $1a_{1u}(\pi)\rightarrow 4eg(\pi^*)$ | |
| | | 17.5 | $3a_{2u}(\pi)\rightarrow d_{z^2}$ | CT |
| | | 2.0 | $3a_{2u}(\pi)\rightarrow d_{x^2-y^2}$ | |
| 27 800 | 0.45/$xy$ | 29.8 | $3a_{2u}(\pi)\rightarrow 4eg(\pi^*)$ | $\pi\rightarrow\pi^*$ |
| | | 20.4 | $3eg(\pi)\rightarrow 4eg(\pi^*)$ | |
| | | 12.5 | $1a_{1u}(\pi)\rightarrow 4eg(\pi^*)$ | |
| | | 7.0 | $3a_{2u}(\pi)\rightarrow d_{z^2}$ | CT |
| | | 2.0 | $3a_{2u}(\pi)\rightarrow d_{x^2-y^2}$ | |
| | | 2.0 | $3eg(\pi)\rightarrow d_{z^2}$ | |
| 28 512 | 0.14/$xy$ | 54.5 | $3eg(\pi)\rightarrow 4eg(\pi^*)$ | $\pi\rightarrow\pi^*$ |
| | | 2.7 | $3a_{2u}(\pi)\rightarrow 4eg(\pi^*)$ | |
| | | 2.3 | $1a_{1u}(\pi)\rightarrow 4eg(\pi^*)$ | |
| | | 14.9 | $3eg(\pi)\rightarrow d_{x^2-y^2}$ | CT |
| | | 7.1 | $3eg(\pi)\rightarrow d_{z^2}$ | |

The results obtained also allow us to determine the causal relationship between a spin-state change and a shift in Soret band frequency. As mentioned above, the early hypothesis advanced was that a blue shift in the high-spin state is due to enhanced mixing of charge-transfer excitations in the Soret band. However, an examination of the results in Tables I and II indicates that this is not the case. The most intense bands in the high-spin spectrum at 30 129, 30 322, 30 924, and 31 179 cm$^{-1}$ contain no more than 6% charge-transfer excitation character. The most intense bands in the low-spin spectrum, at 27 418, 27 800, and 28 512 cm$^{-1}$, contain 10–20% charge-transfer excitations. Thus, the charge-transfer character of the most intense B-bands in the low-spin ground-state spectrum are higher than those in the high-spin ground-state spectrum. This result directly contradicts Braterman's early speculation that it was charge-transfer excitations mixing with $1a_{1u},3a_{2u}\rightarrow eg(\pi^*)$ excitations in the high-spin form, and absent in the low-spin form, that resulted in a blue-shifted B-band in the high-spin spectrum.

The origin of the blue shift in the Soret Band can be seen in the orbital energy diagram for the high- and low-spin states of the model substrate-free P450$_{cam}$ active site, shown in Figure 3. As seen in this figure, the $1a_{1u}(\pi)$,$3a_{2u}(\pi)$, and $3eg(\pi)$ orbitals

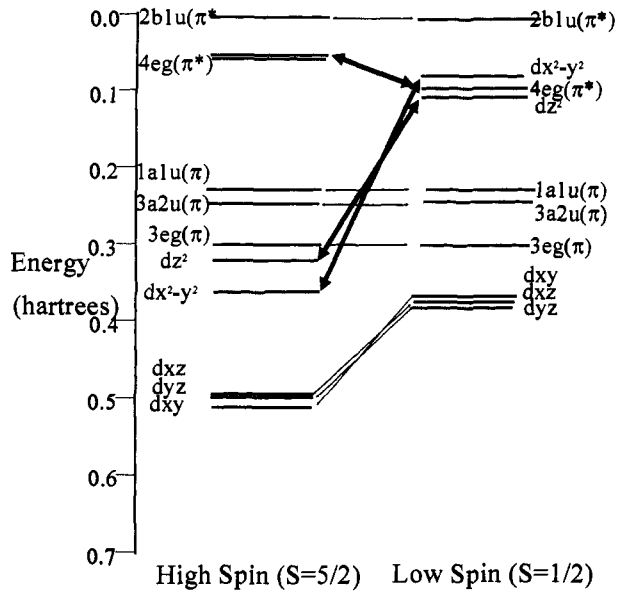


**Figure 3.** Energy diagram for porphyrin $\pi$ and iron d orbitals for the model ferric P450$_{cam}$ active site in a high- and a low-spin state.

**Table III.** Percentage of $d_{z^2}/d_{x^2-y^2}$ Character in Porphyrin eg($\pi^*$) Orbitals for High- and Low-Spin Ferric Heme

| percentage high-spin eg($\pi^*$) | | percentage low-spin eg($\pi^*$) | |
|---|---|---|---|
| $d_{z^2}$ | $d_{x^2-y^2}$ | $d_{z^2}$ | $d_{x^2-y^2}$ |
| 0.00/0.02 | 0.02/0.00 | 0.18/1.67 | 1.63/0.04 |

are relatively unaffected by the Fe(III) spin-state change. However, there is a substantial increase in the energy of the unoccupied 4eg($\pi^*$) orbitals in going from low to high spin. Thus, the orbital separation between the $\pi$ and $\pi^*$ orbitals that contribute the main excitation to the Soret band is increased in the high-spin state, directly accounting for the observed increase in the energy of that transition.

The question still remains as to what causes the change in energy of the unoccupied 4eg($\pi^*$) orbital between the high- and low-spin states, since the relationship between the porphyrin $\pi^*$ orbital energy shift and the change in spin state of the iron is not intuitively obvious. The answer lies in the shift in energies of the d orbitals in the two states, as shown in Figure 3, and the enhanced interaction with the porphyrin $\pi^*$ orbital in the low-spin state, as shown in Table III. As seen in Figure 3, in the low-spin state, the iron d orbitals increase in energy and the splitting between the $t_{2g}$ ($d_{xy}$, $d_{xz}$, $d_{yz}$) and eg ($d_{x^2-y^2}$, $d_{z^2}$) orbitals decreases compared to the high-spin state. As shown in Table III, this shift causes a significant mixing of $d_{z^2}$ and $d_{x^2-y^2}$ orbitals with porphyrin ring atom $p_z$ orbitals in the eg($\pi^*$) molecular orbitals, a mixing that is absent in the high-spin state. This mixing lowers the energy of the 4eg($\pi^*$); the iron $d_{z^2}$ and $d_{x^2-y^2}$ and porphyrin 4eg($\pi^*$) orbitals become nearly degenerate, and the energy separation between the 4eg($\pi^*$) and the $1a_{1u}(\pi)$ and $3a_{2u}(\pi)$ orbitals is decreased. Since transitions between the $a_{1u}$ and $a_{2u}$ and the 4eg($\pi^*$) are a major contribution to the Soret band, the lower energy of the 4eg($\pi^*$) orbitals leads to a red-shifted Soret band in the low-spin state.

## Conclusions

The calculated electronic structure and spectra of a model substrate-free ferric P450$_{cam}$ active site in a high ($S = {}^5/_2$) and a low ($S = {}^1/_2$) spin state provide, for the first time, a direct mechanistic link between a shift in the Soret band and a change in iron spin state. The results obtained clearly indicate that a mere spin-state change from low to high spin, for a fixed-geometry ferric heme–aquo–methyl mercaptide system, results in a blue shift in the Soret band. Moreover, the origin of this shift has also been identified as the result of a lowering of the 4eg($\pi^*$) porphyrin orbitals due to mixing with the $d_{z^2}$ and $d_{x^2-y^2}$ ferric ion orbitals in the low-spin state. This mixing is, in turn, caused by an increase in these d orbital energies as a direct consequence of the iron spin-state change bringing them closer to the 4eg($\pi^*$) porphyrin orbitals in the low-spin state. Taken together, then, the following mechanistic link between spin-state change and Soret band frequency emerges: (i) a change in occupancy of the d orbitals in the two spin states affects the relative energies of the d orbital; (ii) the increased energy of the unoccupied $d_{z^2}$ and $d_{x^2-y^2}$ orbitals in the low-spin state allow them to substantially interact with the 4eg($\pi^*$) orbital, lowering its energy (this interaction does not occur in the high-spin state); and (iii) the energy of the occupied $1a_{1u}$ and $3a_{2u}$ orbitals is unaffected. Thus, the energy difference between the four main molecular orbitals involved in the Soret transition is lowered in the low-spin state, shifting the band to the red. This process forms the underlying physical basis for the observed correlations between ferric heme spin state and measured spectra associated with ($\pi \rightarrow \pi^*$) heme transitions. The correlation between Soret band shift and high-/low-spin percentage can now be used with increased confidence in its validity, even in the absence of independent evidence for a change in spin state.

**Acknowledgment.** Support for this work from NIH Grant GM27943 is gratefully acknowledged. The authors also thank Dr. Ping Du and Dr. Jack Collins for helpful comments.